

SONIFICATION OF OF KEPLER FIELD SU UMA CATAclySMIC VARIABLE STARS V344 LYR AND V1504 CYG

ROXANNE M. TUTCHTON^{1,2}, MATT A. WOOD³, MARTIN D. STILL^{4,5}, STEVE B. HOWELL⁵,
 JOHN K. CANNIZZO^{6,7} & ALAN P. SMALE⁸

ABSTRACT

Sonification is the conversion of quantitative data into sound. In this work we explain the methods used in the sonification of light curves provided by the *Kepler* instrument from Q2 through Q6 for the cataclysmic variable systems V344 Lyr and V1504 Cyg. Both systems are SU UMa stars showing dwarf nova outbursts and superoutbursts as well as positive and negative superhumps. Focused sonifications were done from average pulse shapes of each superhump, and separate sonifications of the full, residual light curves were done for both stars. The audio of these data reflected distinct patterns within the evolutions of supercycles and superhumps that matched previous observations and proved to be effective aids in data analysis.

Subject headings: accretion disks; cataclysmic variables; dwarf novae; methods: miscellaneous; stars individual (V344 Lyr, V1504 Cyg)

1. INTRODUCTION

NASA's Discovery mission *Kepler* has yielded observational data of unprecedented quality for numerous astronomical objects. Among the benefits consequent of this is the ability to explore methods of data representation such as sonification; the conversion of quantitative data into sound. This report focuses on the methods and characteristics of the auditory representations of *Kepler* light curve data from the SU UMa cataclysmic variable systems V344 Lyr and V1504 Cyg.

Cataclysmic variable (CV) binaries are composed of a low-mass secondary star (M_2) that transfers material through the inner Lagrange point to a more massive white dwarf primary (M_1) by way of an accretion disk, which dominates the magnitude of the entire system (Wood et al. 2011). Dwarf novae (DN) are a subclass of CV that display outbursts on a recurrent time scale specific to each system. They are arguably the most valuable systems in the study of accretion disks (Warner 1995a; Hellier 2001).

SU UMa stars are a type of dwarf nova CV that, in addition to normal DN outbursts, also display periodic superoutbursts that are ~ 0.7 magnitudes brighter and four to five times longer than DN outbursts. During superoutbursts these stars also display hump-shaped distortions in the accretion disk called positive superhumps (Warner 1995a; Hellier 2001). These positive superhumps oscillate

at a slightly longer period than the orbital period of the system. They are called 'positive' due to the definition of the fractional period excess:

$$\epsilon_+ \equiv \frac{P_+ - P_{orb}}{P_{orb}}, \quad (1)$$

where P_+ is the positive superhump orbit and an P_{orb} is the orbital period of the binary. Figure 1 shows a simulated cycle of a positive superhump where frames 1 and 6 show the disk at its maximum compression (see, e.g., Wood et al. 2009).

Superoutbursts appear to begin as DN outbursts (see Cannizzo et al. 2010, 2012). During quiescence the viscosity of the accretion disk is low, and matter is transmitted at a higher rate through the inner Lagrange point than it is incorporated into the primary. Thus material accumulates until the disk transitions to a high-viscosity state and spreads inward and/or outward increasing in radius. After several of these DN outbursts the outer radius of the disk reaches 3:1 co-rotation resonance where the Keplerian disk material orbits three times for every orbital cycle. This is only possible in systems with a mass ratio $q = M_2/M_1 \lesssim 0.35$ (Wood et al. 2009; Hellier 2001).

During the peak of the superoutburst when sufficient mass in the outer disk is ionized, superhumps form, increasing tidal stresses and angular momentum. At this point the periodic compression of the accretion disk opposite the secondary star is the source of the superhump signal (Figure 1), so we call these *disk* superhumps. During the superoutburst maximum, the disk superhumps dominate the light curve, but as these fade as a result of mass draining from the disk, a second anti-phased signal with the same period becomes evident. This second signal results from the impact of the accretion stream on the rim of the non-axisymmetric, oscillating disk. When the stream impacts deeper in the potential well of the primary, more specific kinetic energy is dissipated and the spot is brighter. These are *stream* superhumps, or what have been called *late* superhumps in the literature. The

Electronic address: roxannetutchton@coloradocollege.edu

¹ Department of Physics, Colorado College, 14 East Cache La Poudre Street, Colorado Springs, CO 80903

² Southeastern Association for Research in Astronomy (SARA) NSF-REU Summer Intern

³ Department of Physics and Space Sciences, Florida Institute of Technology, FL, 32901

⁴ NASA Ames Research Center, Moffett Field, CA 94095, USA

⁵ Bay Area Environmental Research Institute, Inc., 560 Third St. West, Sonoma, CA 95476, USA

⁶ CRESST and Astroparticle Physics Laboratory NASA/GSFC, Greenbelt, MD 20771, USA

⁷ Department of Physics, University of Maryland, Baltimore County, 1000 Hilltop Circle, Baltimore, MD 21250, USA

⁸ NASA/Goddard Space Flight Center, Greenbelt, MD 20771, USA

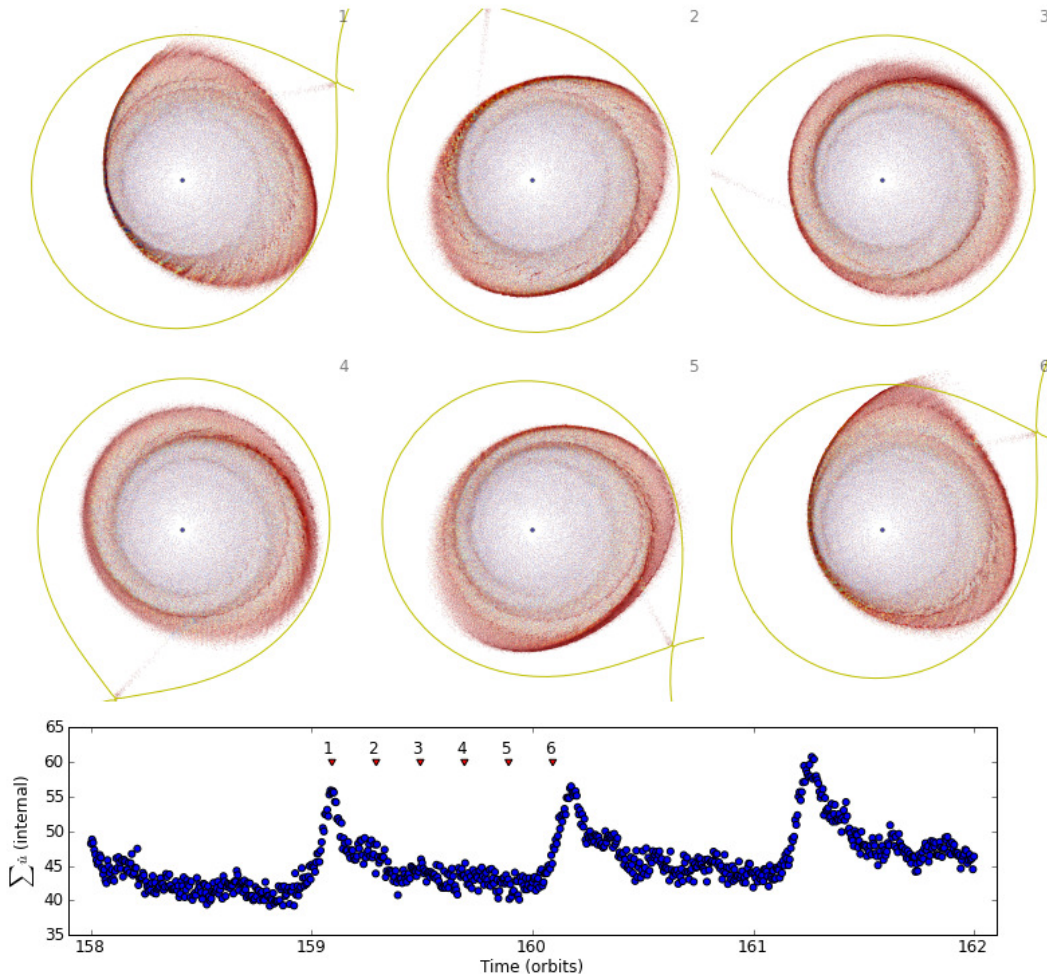


FIG. 1.— Smoothed particle hydrodynamics simulations of one orbit of positive superhumps (Wood et al. 2009). The simulation light curve calculated as the sum of the luminosities of all particles (Wood et al. 2011).

signal from the stream/late superhumps can last well after the disk has returned to a quiescent state (Still et al. 2010) as long as the disk is still flexing. This is the *two-source model of positive superhumps*, and it has been simulated and explained in detail by Wood et al. (2011).

Negative superhumps are photometric signals with a period a few percent shorter than P_{orb} . The period deficit is defined as

$$\epsilon_- \equiv \frac{P_{orb} - P_-}{P_{orb}}, \quad (2)$$

where P_- is the period of the negative superhump. Smoothed particle hydrodynamics (SPH) simulations have shown that negative superhump signals occur when the accretion disk tilts out of the orbital plane, because in this situation the accretion stream impacts region sweeps across the face of the accretion disk along the line of nodes, rather than just impacting the the outer rim. The negative superhump maximum occurs when the accre-

tion stream impact point is deepest in the potential well of the primary (Wood et al. 2011). These phenomena have been observed in several types of CV's, sometimes simultaneously with positive superhumps as is the case with both V344 Lyr and V1504 Cyg.

V344 Lyr is one of 16 known cataclysmic variables in the Kepler field. It was classified as an SU UMa star when observed in superoutburst ($V \sim 14$) by Kato (1993). This observation revealed positive superhumps with a period of 2.1948 ± 0.0005 hr. Further study showed a DN outburst cycle of 16 ± 3 days and a supercycle of ~ 110 days (Still et al. 2010). Wood et al. (2011) determined the orbital period of V344 Lyr to be $2.109696 \pm 7 \times 10^{-5}$ hr. The mean positive superhump period was reported at $2.20245(8)$ hr and the negative superhump period at 2.06273 ± 0.00005 hr. However, the report noted that the superhump periods drift significantly during superoutburst and that the formal errors are not to be taken literally. The rates of period change for both negative and positive superhumps in V344 Lyr are discussed in

depth by Wood et al. (2011).

V1504 Cyg is also an SU UMa CV. Its orbital period was reported at 1.67 hr in Table 1 of Still et al. (2010), and the Guide Star Catalog puts its quiescent magnitude at $V \sim 18$. The Fourier transform of Q2-Q6 (Figure 3) for the system shows a P_+ of 1.73 hr (13.9 cycles/day) and a P_- of 1.63 hr (14.7 cycles/day). The analysis of the data for this system as well as that of V344 Lyr is expanded in Cannizzo et al. (2012).

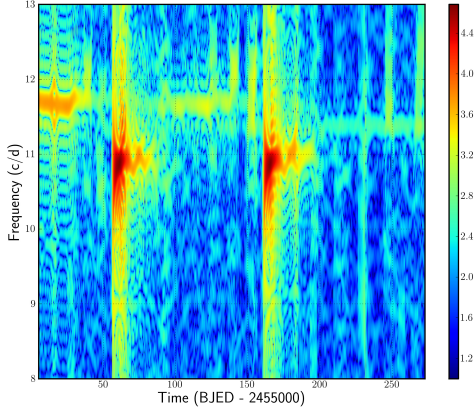


FIG. 2.— The 2D Fourier transform of Q2 and Q3 of V344 Lyr. The figure shows the first two superoutbursts as well as the negative superhump at the beginning of Q2.

1.1. The Kepler Mission

Kepler's primary mission is to observe multiple targets in order to detect terrestrial planets within the habitable range of solar-type stars. The mission was launched into a 372.5 d, earth-trailing, heliocentric orbit on 2009 March 6. *Kepler* has a 0.95 m Schmidt camera with a field of view spanning 116 square degrees, which is focused on a field with low Galactic latitude (Haas et al. 2010). This field of view also contains other objects of astrophysical interest, including at least 16 CV's, 10 of which are listed in Table 1 of Still et al. (2010).

The *Kepler* instrument can observe targets with both a long cadence (LC) sampling interval of 29.4 min and a short cadence (SC) interval of 58.8 s. Data from these targets is available from the Science Operations Center in reduced and calibrated form after propagation through the standard data reduction pipeline.

2. SONIFICATION METHOD

During Q2-Q6 both V344 Lyr and V1504 Cyg showed four superoutbursts with positive superhumps. These phenomena, along with the negative superhumps, were the focus of the sonification process. A high pass filter was applied to the SAP (simple aperture photometry) light curves (Figure 4) to remove the large-amplitude dwarf nova outburst and superoutburst behavior in order to isolate the superhump signal (Figure 5). This was done by subtracting a boxcar-smoothed profile curve with a window width the same length as the superhump period. The positive superhumps were then isolated, and thirty average pulse shapes were taken from the ~ 15 d residual data using two day windows (roughly twice the beat period of the positive and negative superhumps).

Four-day windows were used for the negative superhumps due to their longer duration.

Folding frequencies (f_{fold}) of the average pulse shapes were found by searching the superhump frequency ranges in Fourier amplitude spectra. The range for the positive superhumps in V344 Lyr was between 10-12 cycles/day and 13-15 cycles/day for V1504 Cyg (Figures 2 and 3). In the event of negative superhump interference the frequency range was lowered to filter the negative superhump signal out of the positive superhump pulse shapes. Negative superhumps were processed separately using a frequency range of 11.5-12 cycles/day and 14.6-15 cycles/day for V344 Lyr and V1504 Cyg respectively. Table 1 gives the parameters for each systems' sonification process.

The 'period', or number of points in the cycles of each pulse shape, was determined by the expression

$$n_{bins} = \frac{n_{bins\phi} \times P_{fold} \times 24hrs}{P_{\pm}}, \quad (3)$$

where $n_{bins\phi}$ is a chosen parameter that sets the initial period range of the pulse shapes and, therefore, the absolute tonal range of the sonification (Table 1); P_{fold} is the fold period ($1/f_{fold}$) for the average pulse shape; and P_{\pm} is the positive or negative superhump period for the system being sonified. The periods of the positive and negative superhumps for V344 Lyr and V1504 Cyg along with their orbital periods, which have been determined by previous observation, are given in Table 2.

Each average pulse shape was extended until it contained 11025 points. This yielded 30 distinct pulse shapes with frequencies determined from the observed superhump periods. These pulse shapes were recombined by first normalizing and shifting them to a unified zero before clipping each one into a standard sine wave. Then the pulse shapes were returned to their original amplitudes, and a linear weighting function of the form

$$w = 1 - \frac{i}{2 \times n_{bins}} \quad (4)$$

was used to phase the last two cycles of the preceding chunk with the first two cycles of the next one to create a smooth transition from one pulse shape to the next. In the above expression, i is each index point in the average pulse shape from its beginning to $i = 2 \times n_{bins}$ (see Equation 3).

Once the average pulse shapes were recombined they were processed into a 30 second uncompressed WAV file with a sample rate of 11025 Hz. Changing the sample rate alters the pitch range of the file. The smaller the sample rate, the lower the relative pitch of each pulse shape. The tempo of the file could be changed by altering either the sample rate in the WAV file or the number of points in each pulse shape. For example specifying the number of points in each shape to be 11025 but letting the sample rate of the WAV file be 22050 Hz will result in a sound twice as fast, half as long, and an octave higher than one in which the number of points and the sample rate are both 11025. The volume of each file depends on the magnitude of the signals in the light curve. These amplitudes were modified to fit the $\sim 32,000$ signed 16-bin count capacity of a standard WAV.

In addition to the focused sonifications of the super-

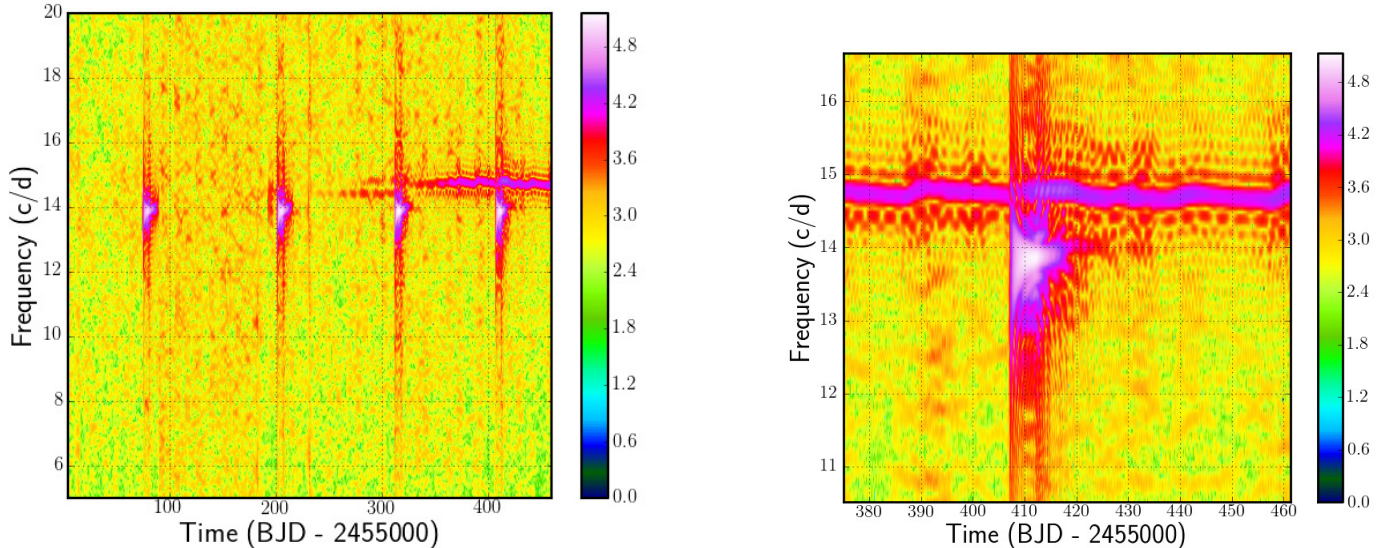


FIG. 3.— Left: The 2D Fourier transform of Q2-Q6 data for V1504 Cyg. Right: A close up view of positive superhump 4 and the negative superhump signal.

TABLE 1
SUPERHUMP SONIFICATION PARAMETERS FOR V344 LYR AND V1504 CYG.

| Star | $n_{bins\phi}$ | Superhump | Duration (BJD-2455000) | Frequency Range (c/d) | Pulse-shape window (days) |
|-----------|----------------|-----------|---------------------------|--------------------------|------------------------------|
| V344 Lyr | 100 | 1 | 58- 74 | 10.0-11.3 | 2 |
| | | 2 | 162-178 | 10.0-11.3 | 2 |
| | | 3 | 278-295 | 10.0-12.0 | 2 |
| | | 4 | 400-416 | 10.0-12.0 | 2 |
| | | Negative | 2- 43 | 11.5-12.0 | 4 |
| V1504 Cyg | 120 | 1 | 75- 90 | 13.0-14.5 | 2 |
| | | 2 | 201-216 | 13.0-14.5 | 2 |
| | | 3 | 312-327 | 13.0-14.5 | 2 |
| | | 4 | 406-422 | 13.0-14.2 | 2 |
| | | Negative | 334-462 | 14.6-15.0 | 4 |

NOTE. — Table 1 lists the parameters for the sonifications of each each superhump during Q2-Q6 of V344 Lyr and V1504 Cyg. All superhump sonifications are ~ 29 seconds in length except for the negative superhump in Q6 of V1504 Cyg, which is ~ 43 seconds.

TABLE 2
PHYSICAL CHARACTERISTICS OF V344 LYR AND V1504 CYG.

| Star | Kepler ID | α (J2000) | δ (J2000) | P_{orb} (hr) | P_+ (hr) | P_- (hr) |
|-----------|-----------|------------------|------------------|----------------|------------|------------|
| V344 Lyr | 7659570 | 18 44 39.17 | +43 22 28.2 | 2.11 | 2.20 | 2.06 |
| V1504 Cyg | 7446357 | 19 28 56.47 | +43 05 37.1 | 1.67 | 1.73 | 1.63 |

NOTE. — Table 2 gives the locations and various periods for the stars V344 Lyr and V1504 Cyg

humps from V344 Lyr and V1504 Cyg, a sonification was done for each of the systems' full residual light curves for quarters two through six. Each of these curves contains $\sim 637,000$ points, which yielded 57-sec WAV files when sampled at 11025 Hz. A second sonification of the same curves was done at twice the sample rate in order to compare the two ranges as well as more easily identify the high-pitched overtones of the negative superhumps.

3. RESULTS: PHYSICAL EVENTS AND THEIR AUDIO SIGNATURES

The sonifications of V344 Lyr and V1504 Cyg revealed patterns within the respective light curves. Though every superoutburst is unique, there is repetition in the progression of tones through the superhumps of each system. Furthermore, there are foretelling characteristics in the audio of the full lights curves shortly preceding superoutbursts. All of the sonifications referred to in this report can be found at www.astro.fit.edu/wood/sonifications.

From the beginning of a superoutburst it takes ~ 15 days for the accretion disk in V344 Lyr to return to its

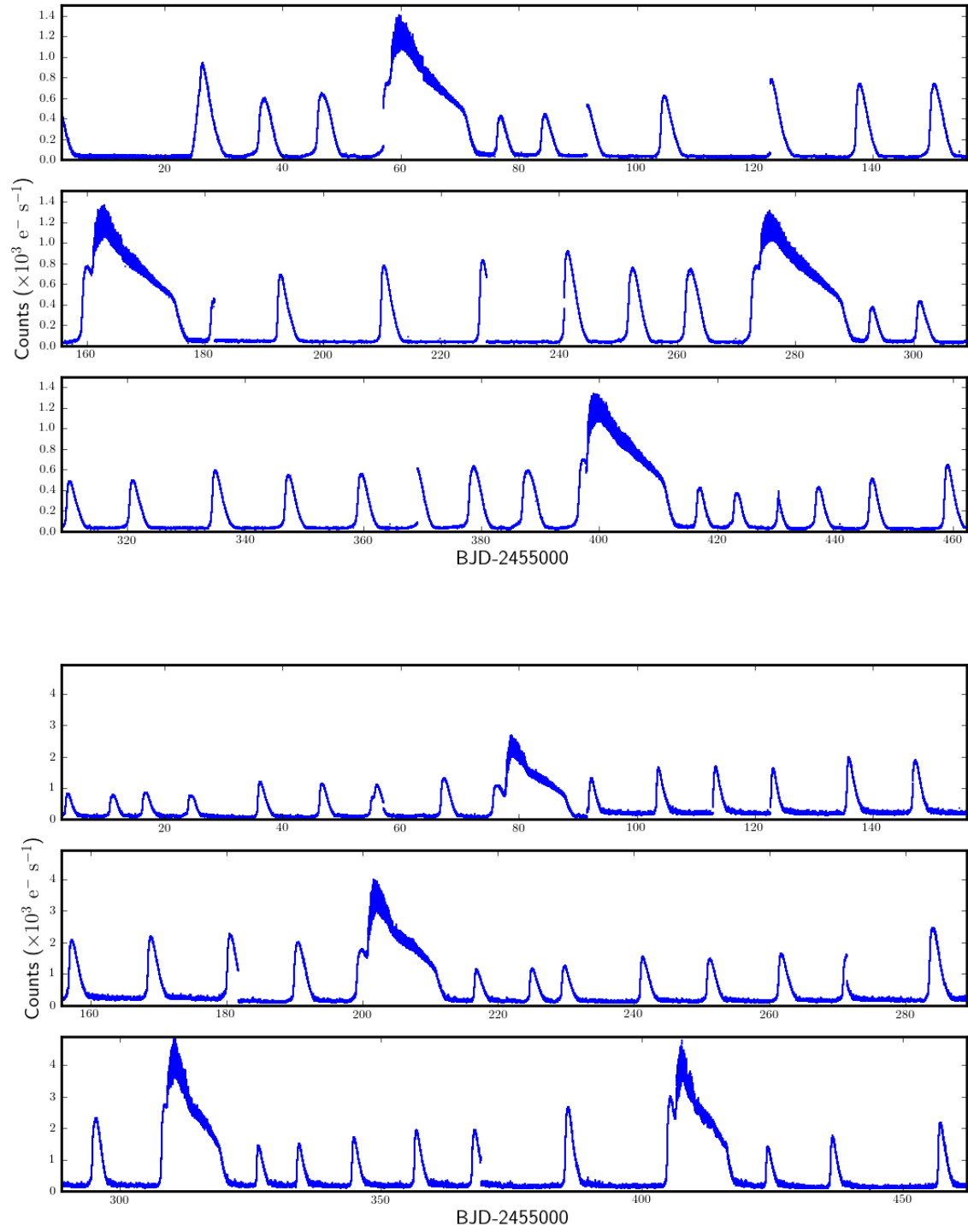


FIG. 4.— Top: The V344 Lyr *Kepler* SAP light curve from Q2-Q6 in photon-counts. Bottom: The V1504 Cyg SAP light curve (Q2-Q6).

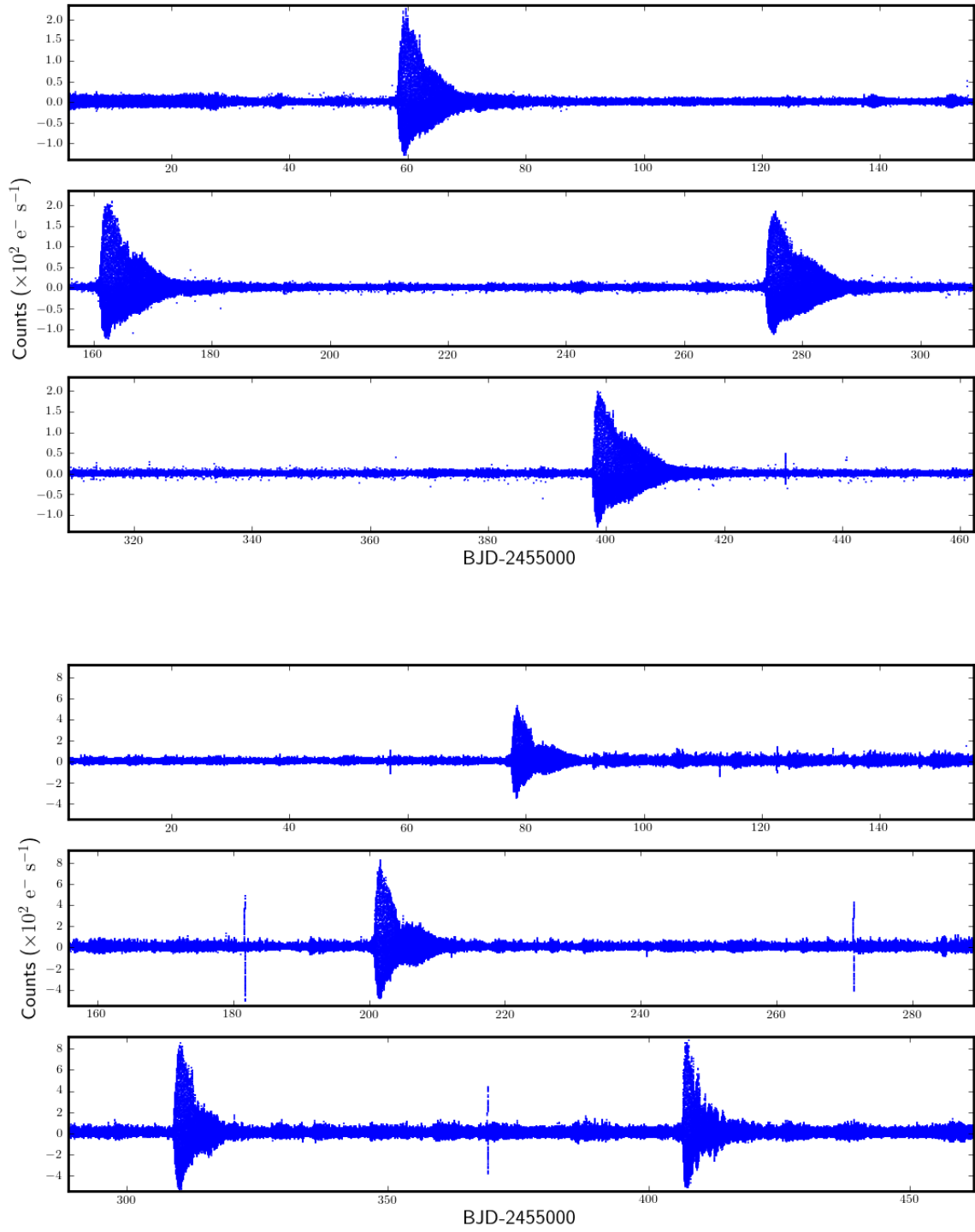


FIG. 5.— Top: The residuals of the *Kelper* Q2-Q6 light curve for V344 Lyr. Bottom: The V1504 Cyg residual light curve (Q2-Q6).

low viscosity state. This occurred four times during Q2-Q6. Wood et al. (2011) reported on the first two superoutbursts of Q2-Q4. Their analysis revealed that both superoutbursts were initiated by DN outbursts. The Fourier transform also revealed the presence of a negative superhump signal at the beginning of the second quarter (Figure 2).

Superoutbursts in V1504 Cyg last ~ 14 days. Like V344 Lyr, four superoutbursts occurred in this system during Q2-Q6 all of which appear to have started as DN outbursts. The Fourier transform showed a negative superhump at the end of Q6 simultaneously with positive superhump 4.

3.1. Positive superhump sonifications

Figure 6 shows the residual light curves for the four superoutbursts from V344 Lyr and V1504 Cyg. Those from V344 Lyr have roughly the same amplitude and overall shape where the superhumps from V1504 Cyg increase in amplitude through the data. The average pulse shapes taken of these superhumps show several reoccurring themes for both systems. The appendix contains the pulse shapes that make up the sonifications of each superhump from V344 Lyr and V1504 Cyg (Figures 7 through 16).

The average pulse shapes for superhump 1 in V344 Lyr start only a few cycles from the saturation point of the superhump (Figure 7). The first four pulse shapes showed signal from the early superhump. They are smooth and sharply peaked with little to no noise. By the fifth or sixth pulse shape, the curve started to develop two distinct local maxima. This is the signal from the late superhump. As explained in Wood et al. (2011), the large peak is the signal from the viscous dissipation in the disk as it oscillations; the second peak is from the bright-spot signal. This shape evolved through the decay of the superhump until the signal from the stream/late superhump dominated and finally modulated back into normal quiescence.

The positive superhumps from V1504 Cyg showed a similar yet unique pattern. Figure 12 displays the average pulse shapes for positive superhump 1 starting ~ 2 days before the beginning of the superhump cycles. The superhump reached its saturation point by the sixth pulse. By the 14th pulse the superhump curve began to display the stream/late superhump signal where the inter pulse peaks are sharper and steeper than those of V344 Lyr. In the last pulse shapes, the noise increased and the curve became a sharply peaked sine wave that appears almost saw-toothed in the ends of superhumps 2 and 3 (Figures 13 and 14).

These progressions are extremely similar for each of the superhumps in the respective systems as is the progression of pitches in the sonified data (www.astro.fit.edu/wood/sonifications). Though the order of tones is not exactly the same in any of the superhumps, the evolution of pitches is so similar in the respective stars that it appears to be characteristic of the system itself. When the sonifications of any two superhumps from the same star are played simultaneously the pitches match up more than half the time. This indicates that the rate of period change of P_+ may be a feature common (or at least very similar) in each superoutburst. This was also mentioned in Wood et al. (2011)'s analysis

of superhumps 1 and 2 of V344 Lyr.

3.2. Negative superhump sonifications

The pulse shapes of the negative superhump in Q2 of V344 Lyr and Q6 of V1504 Cyg have distinct progressions of their own (Figures 11 and 16). Because there was only one occurrence of a negative superhump for each system, no conclusions can be made regarding patterns in negative superhump behavior specific to either V344 Lyr or V1504 Cyg. However, there were several similarities in the superhumps of the different stars.

The apparent characteristic shape of the signal is a flat, slanted portion of the curve to the left of the positive apex. It was the appearance of this shape in positive superhump pulse shapes that lead to the discovery of negative superhump interference in the audio. The frequency range of the pulse shapes was modified to filter the positive and negative superhump signals separately; however, the curves still show some signs of sensitivity to the other's signal.

The sound of the negative superhumps is less dramatic than that of the positive superhumps in both amplitude and pitch variation. The pitch of the superhump changes most drastically in the presence of an outburst. This is clearly seen and heard in the videos of the negative superhumps (www.astro.fit.edu/sonifications). In V344 Lyr when the pulse shape passes over the DN outburst during days ~ 25 to ~ 30 (BJD-2455000) (0:37-0:38), the curve becomes rounder and the pitch slightly lower. By day 34 the negative superhump signal is relatively weak and easily overcome by the signal from a second DN outburst (day 36 to 40) (0:45-0:46).

The pulse shapes of the negative superhump in Q6 of V1504 Cyg were taken from the residual light curve starting on day 334 (BJD-2455000) and continuing to the end of the quarter. Due to the longer duration of this superhump, 45 pulse shapes were taken instead of the usual 30. The most notable deviation from the regular sound of this superhump is during superoutburst 4 from days ~ 406 to ~ 418 (0:45-0:48) during which the amplitude increases substantially and the pitch progression deviates from its previous course.

In general the pulse shapes for V1504 Cyg are shaper and their sounds harsher and louder than those of V344 Lyr. There are also several pulse shapes within the superhumps of both systems that are particularly noisy, which is possibly due to extraneous data or gaps in the light curve that occur when the Kepler instrument adjusts its position (see pulse-shape 25 in Figure 7 or pulse-shape 8 in Figure 14).

3.3. Full sonifications (Q2-Q6)

The sonifications of the full residual light curves are especially revealing because they contain audible signals from each of the superhumps in the time series. Two versions of the sonification were made at sample rates of 11025Hz and 22050Hz for both systems. Table 3 gives a timeline of the events in both sonifications of V344 Lyr and V1504 Cyg.

The superoutbursts, though punctuated by stretches of noise, are easily identifiable in both versions. Faint pulses in the noise can be heard directly preceding each superoutburst. These grow more rapid before the superhump signal overpowers the light curve. The pitches of

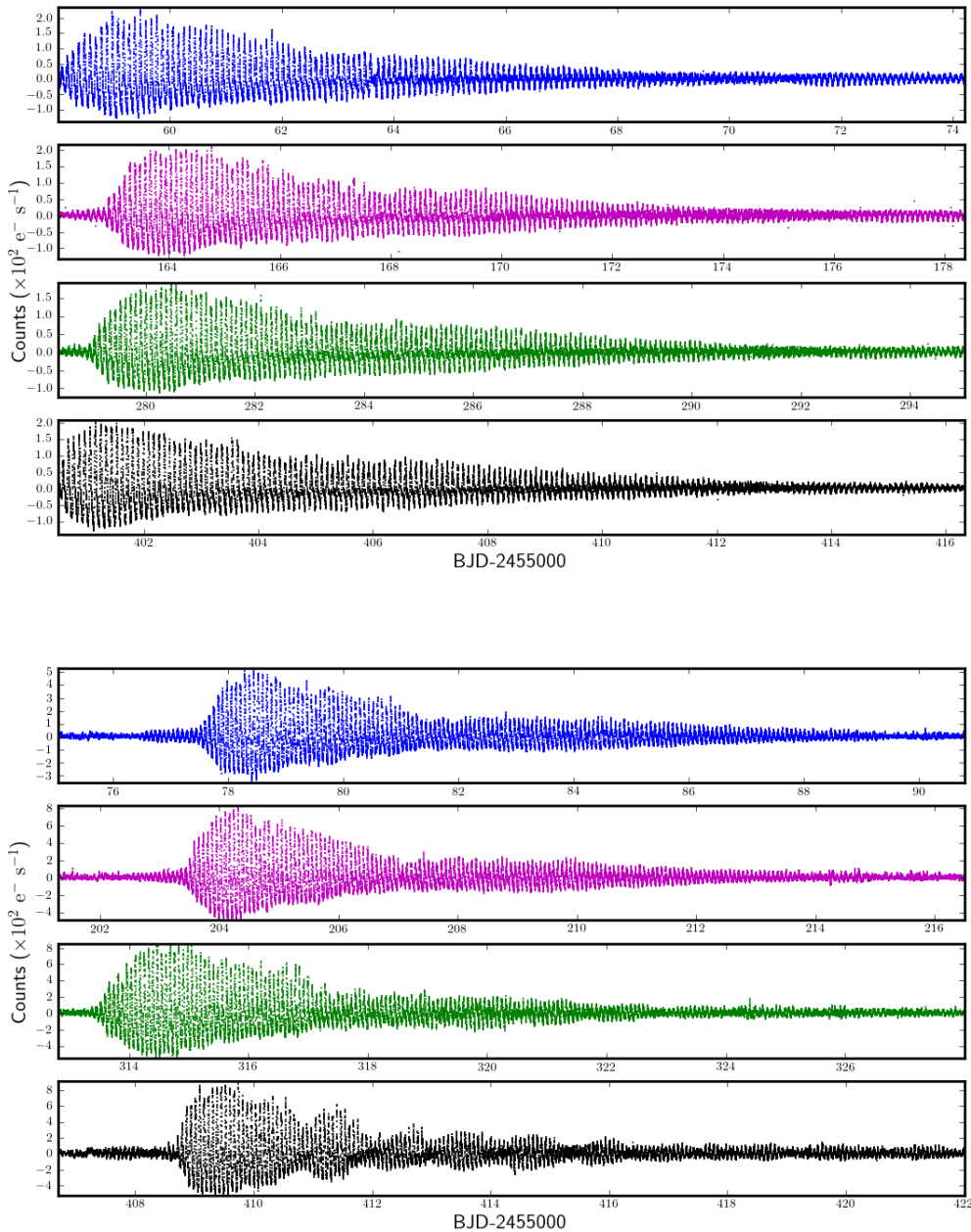


FIG. 6.— The top plot show the four positive superhumps from Q2-Q6 for V344 Lyr taken from the residual light curve, and the bottom plot shows the same for V1504 Cyg.

the full, sonified, light curves are derived directly from the number of points per cycle, so the frequencies are as they would occur if the light curves were 57 seconds long. Thus it makes sense that when compared, the overall pitch of V344 Lyr is lower than that of V1504 Cyg due to the system’s longer period.

The negative superhumps are more difficult to hear in the 11025 Hz files. The volume needs to be turned up significantly in order to identify them. They are more obvious on the files sampled at 22050 Hz. The end of the negative superhump in Q2 of V344 Lyr can be heard at the beginning of the sonifications. It is faint and higher-pitched than the rest of the noise. It last a few seconds

(0:00-0:04) and is indistinguishable by the onset of the first superoutburst. The negative superhump at the end of the V1504 Cyg sonifications is more complete. Its beginning can be heard faintly at $\sim 0:17$, and it grows in magnitude until interrupted at $\sim 0:51$ by superoutburst 4. The Fourier transform of Q2-Q3 for V344 Lyr and Q2-Q6 for V1504 Cyg are helpful visual accompaniments for these sonifications (Figures 2 and 3).

4. CONCLUSION

Sonifications of light curves were successfully created with Kepler time series, photometric data from the stars V344 Lyr and V1504 Cyg. The characteristics of these

TABLE 3
THE EVENT TIMELINE FOR THE FULL Q2-Q6 SONIFICATIONS OF
V344 LYR AND V1504 CYG.

| Star | Event | 11025 Hz file | 22050 Hz file |
|-----------|----------------------|---------------|---------------|
| V344 Lyr | Negative Superhump | 0:00-0:04 | 0:00-0:02 |
| | Positive Superhump 1 | 0:07 | 0:03 |
| | Positive Superhump 2 | 0:20 | 0:10 |
| | Positive Superhump 3 | 0:34 | 0:17 |
| | Positive Superhump 4 | 0:50 | 0:25 |
| V1504 Cyg | Positive Superhump 1 | 0:10 | 0:05 |
| | Positive Superhump 2 | 0:25 | 0:12 |
| | Positive Superhump 3 | 0:39 | 0:19 |
| | Positive Superhump 4 | 0:51 | 0:25 |
| | Negative Superhump | 0:34-0:57 | 0:17-0:28 |

sonifications not only matched previously observed physical phenomenon for the systems, but revealed audible patterns both similar and unique for each star.

The sonifications of the superhumps of each system give a focused representation of portions of the light

curves. These revealed a repeated progression of pitches in the average pulse shapes of the positive superhumps. The relative relationship of these pitches appears to be a unique characteristic of each system. Negative superhumps were also found to have similarities in the behavior of the pulse shapes and sounds common to each star.

Audio of the full residual light curves from Q2-Q6 gives a more general representation of the each system. Both positive and negative superhumps can be heard in these sonifications. There are also distinct pulses in the sound preceding superoutbursts that may be signals from fainter DN outbursts. These audible light curves proved to be accurate representations of events that occurred in the cataclysmic variable SU UMa systems V344 Lyr and V1504 Cyg.

This project was funded by the National Science Foundation Research Experiences for Undergraduates (REU) program through grant NSF AST-1004872.

REFERENCES

- Cannizzo, J. K., Still, M. D., Howell, S. B., Wood, M. A., & Smale, A. P. 2010, *ApJ*, 725, 1393
Cannizzo, J. K., Smale, A. P., Wood, M. A., Still, M. D., & Howell, S. B. 2012, *ApJ*, 747, 117
Haas, M. R., et al. 2010, *ApJ*, 713, L115
Hellier, C. 2001, *Cataclysmic Variable Stars*, Springer, 2001
Still, M., Howell, S. B., Wood, M. A., Cannizzo, J. K., & Smale, A. P. 2010, *ApJ*, 717, L113
Warner, B. 1995a, *Cataclysmic Variable Stars* (Cambridge: Cambridge University Press)
Wood, M. A., Still, M. D., Howell, S. B., Cannizzo, J. K., Smale, A. P. 2011, *ApJ*, 741, 105
Wood, M. A., Thomas, D. M., & Simpson, J. C. 2009, *MNRAS*, 398, 2110

APPENDIX

AVERAGE PULSE SHAPES FOR THE AUDIOIZED SUPERHUMPS IN V344 LYR AND V1504 CYG

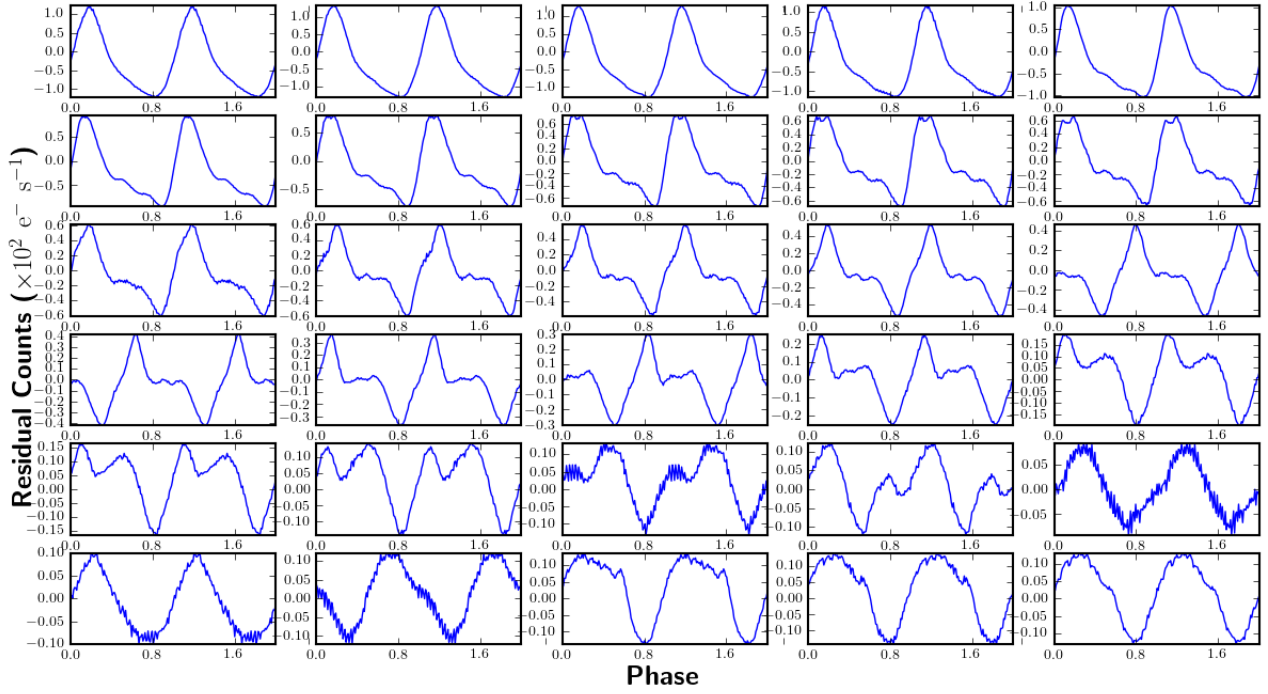


FIG. 7.— Superhump 1 V344 Lyr

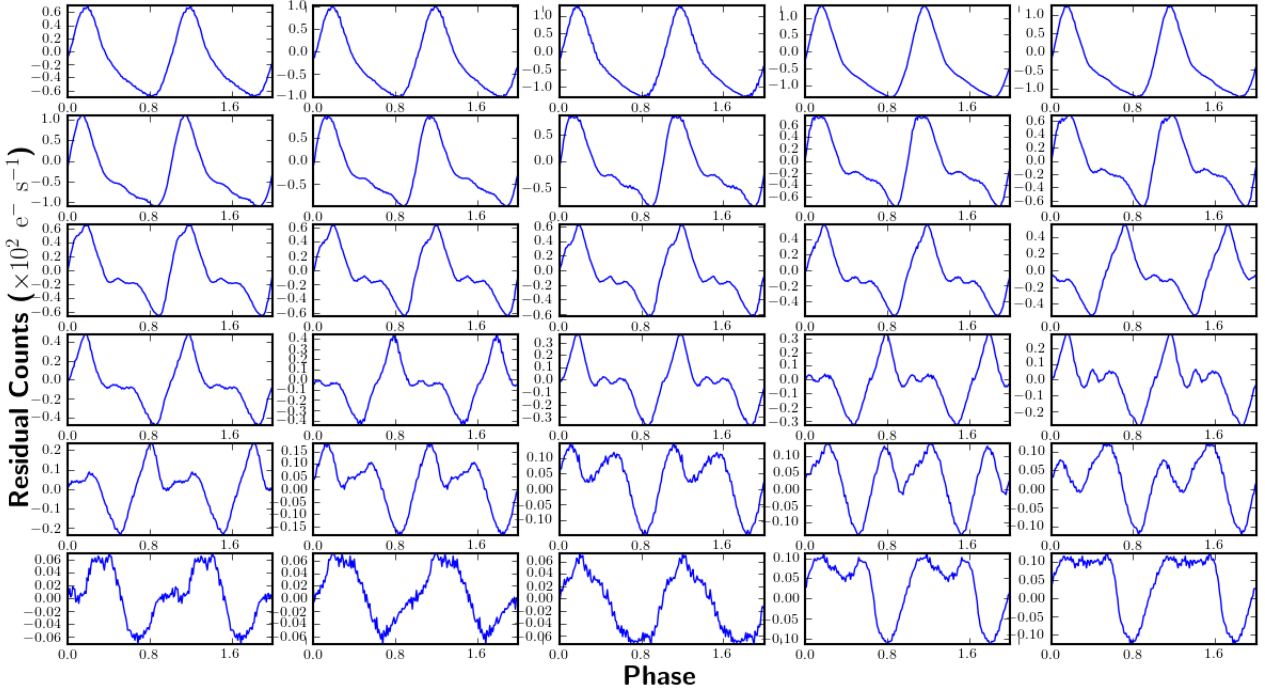


FIG. 8.— Superhump 2 V344 Lyr

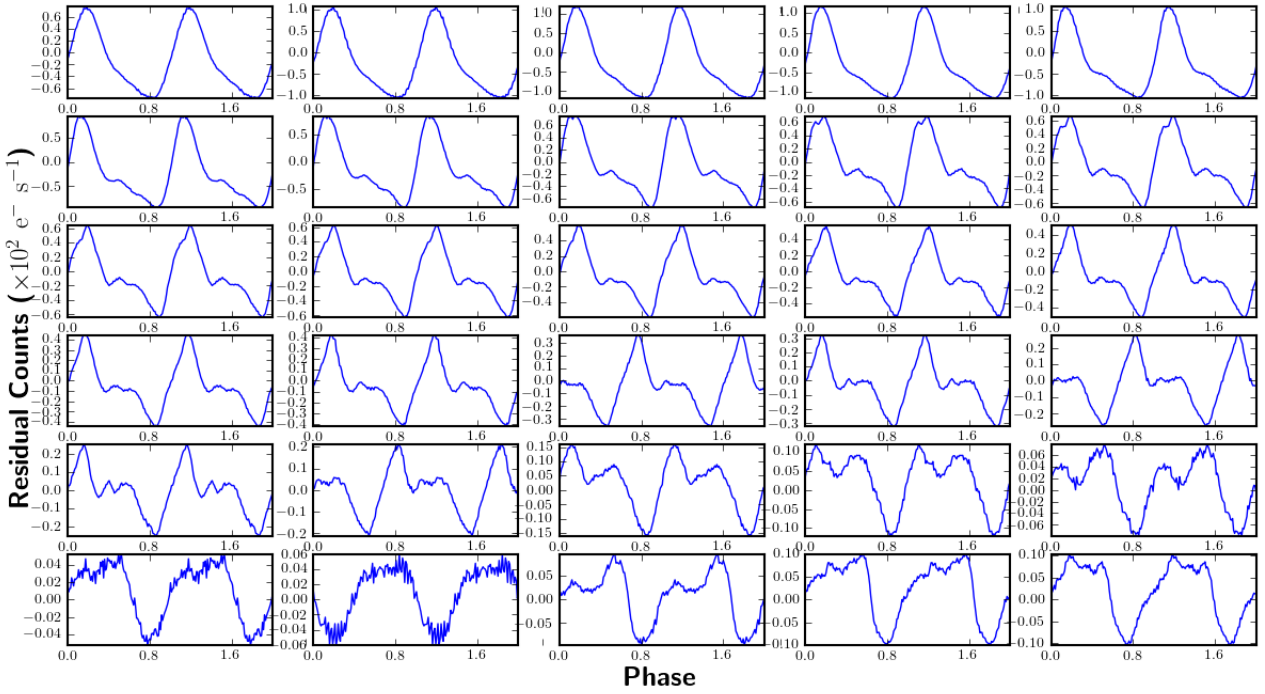


FIG. 9.— Superhump 3 V344 Lyr

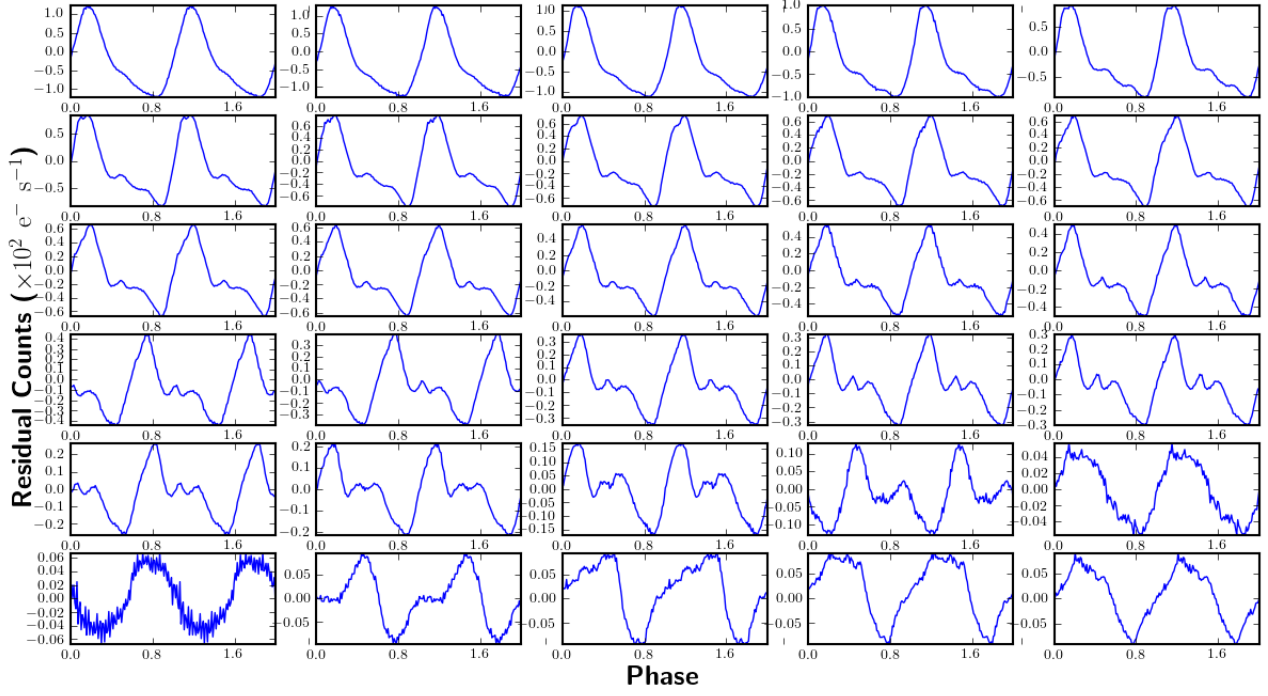


FIG. 10.— Superhump 4 V344 Lyr

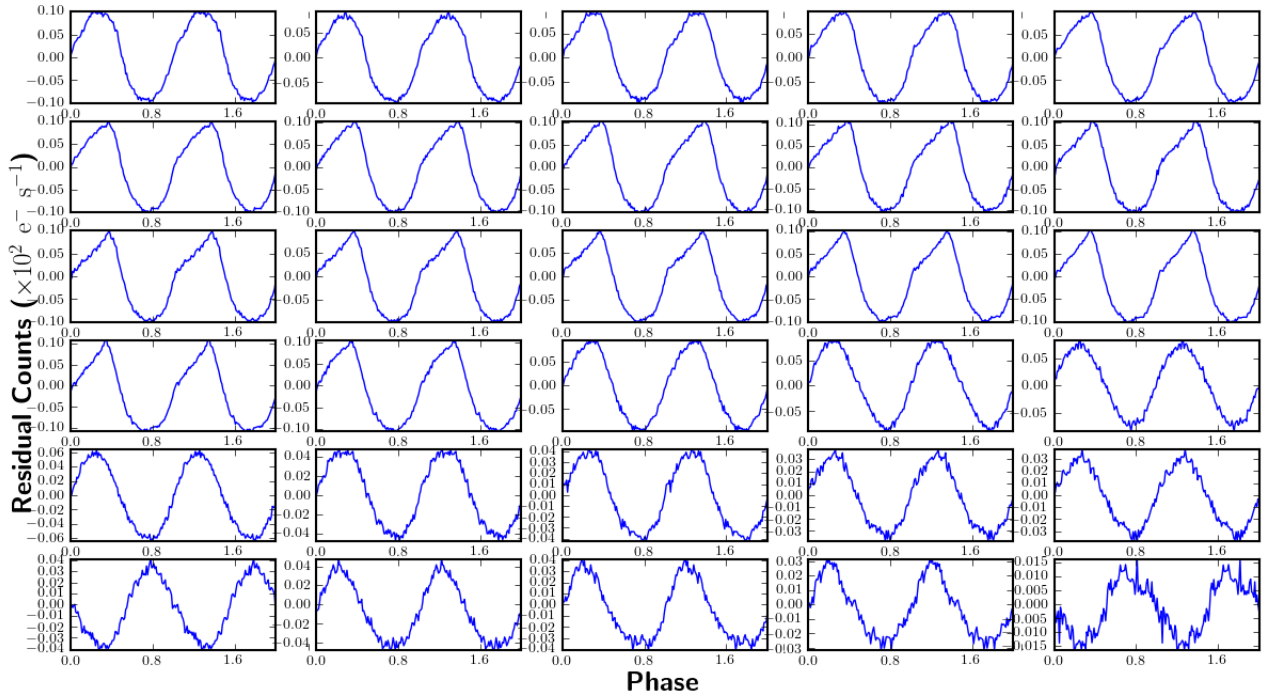


FIG. 11.— Negative superhump (Q2) V344 Lyr

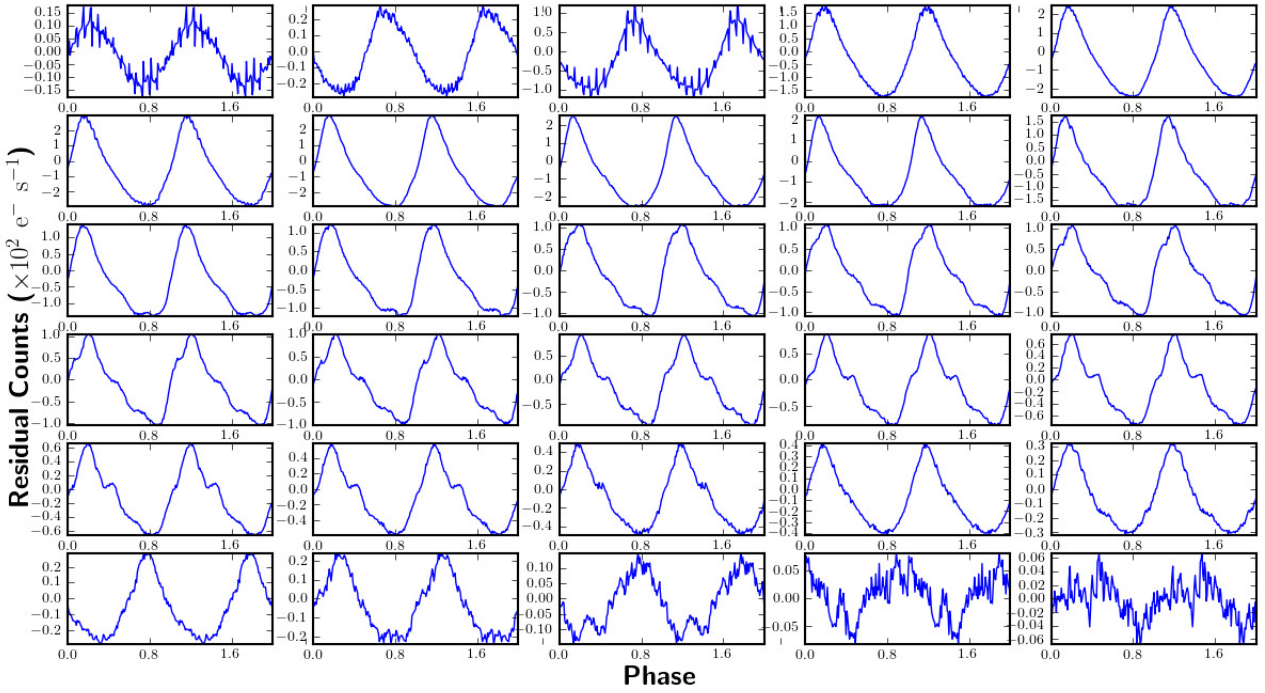


FIG. 12.— Superhump 1 V1504 Cyg

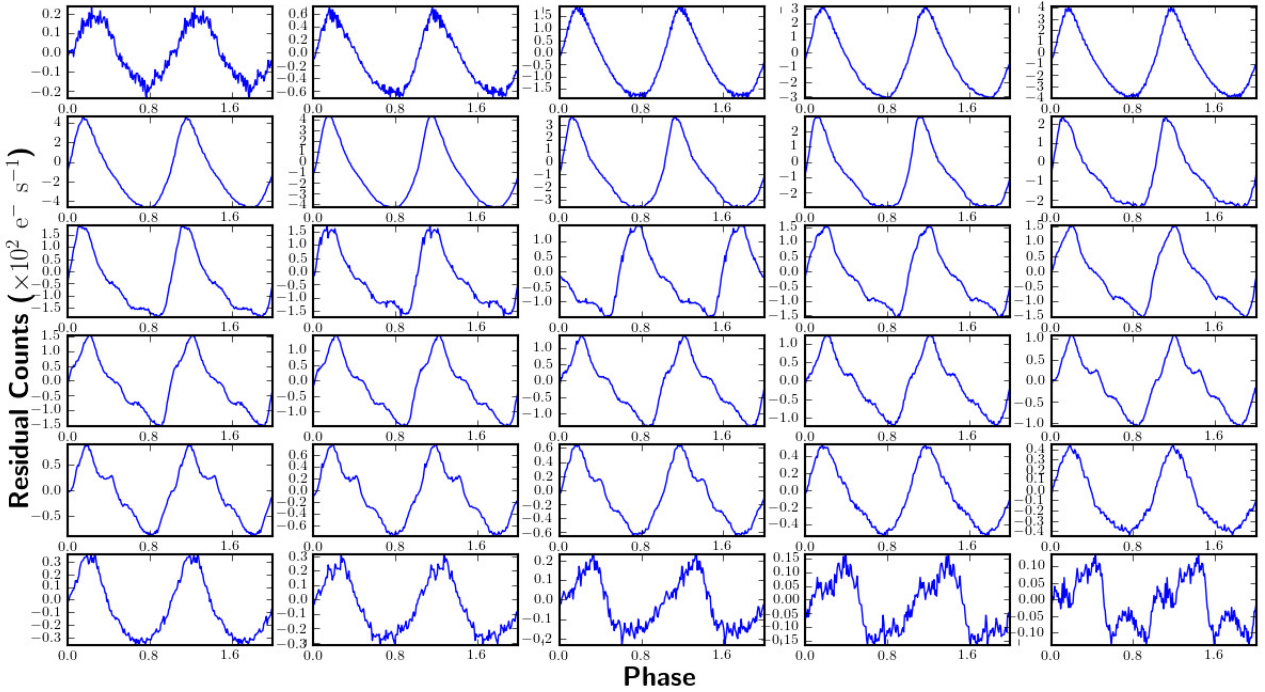


FIG. 13.— Superhump 2 V1504 Cyg

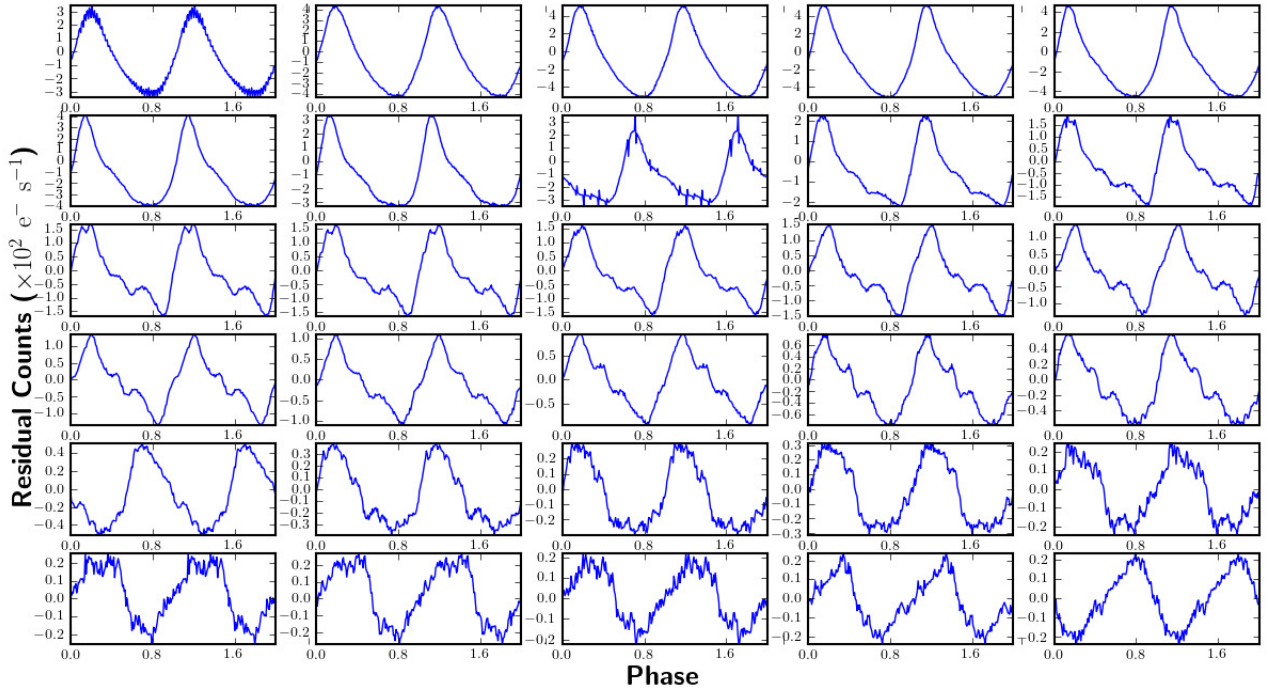


FIG. 14.— Superhump 3 V1504 Cyg

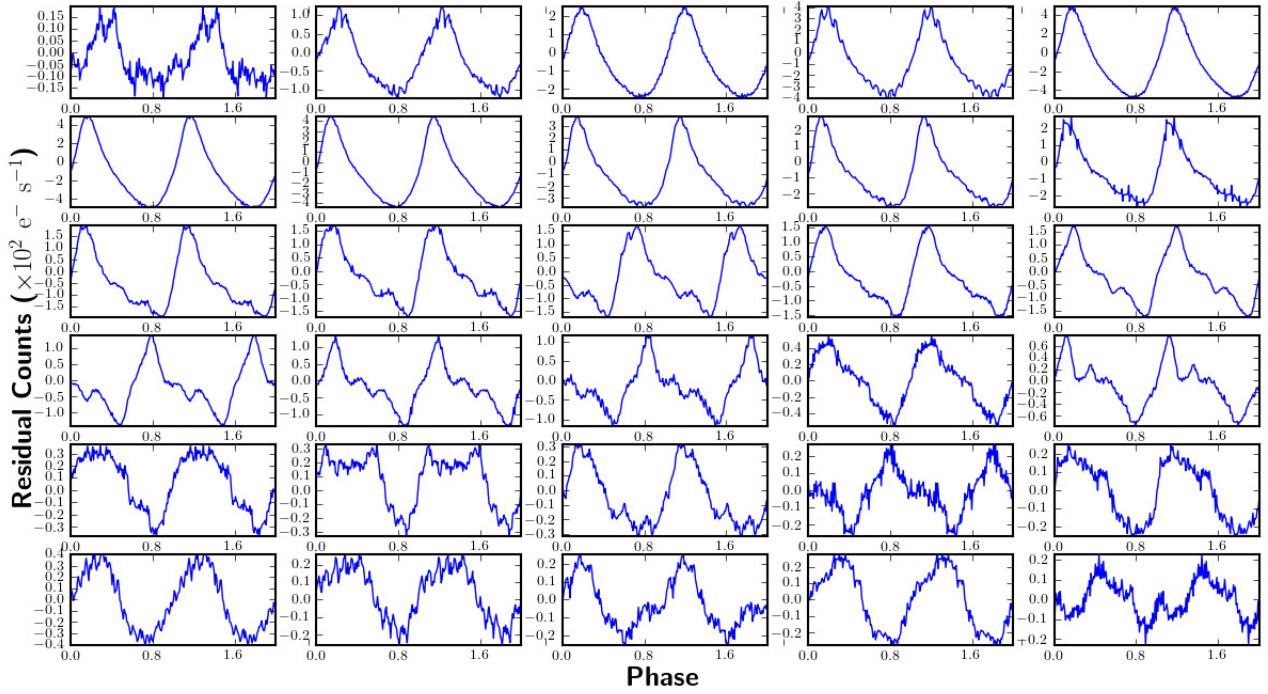


FIG. 15.— Superhump 4 V1504 Cyg

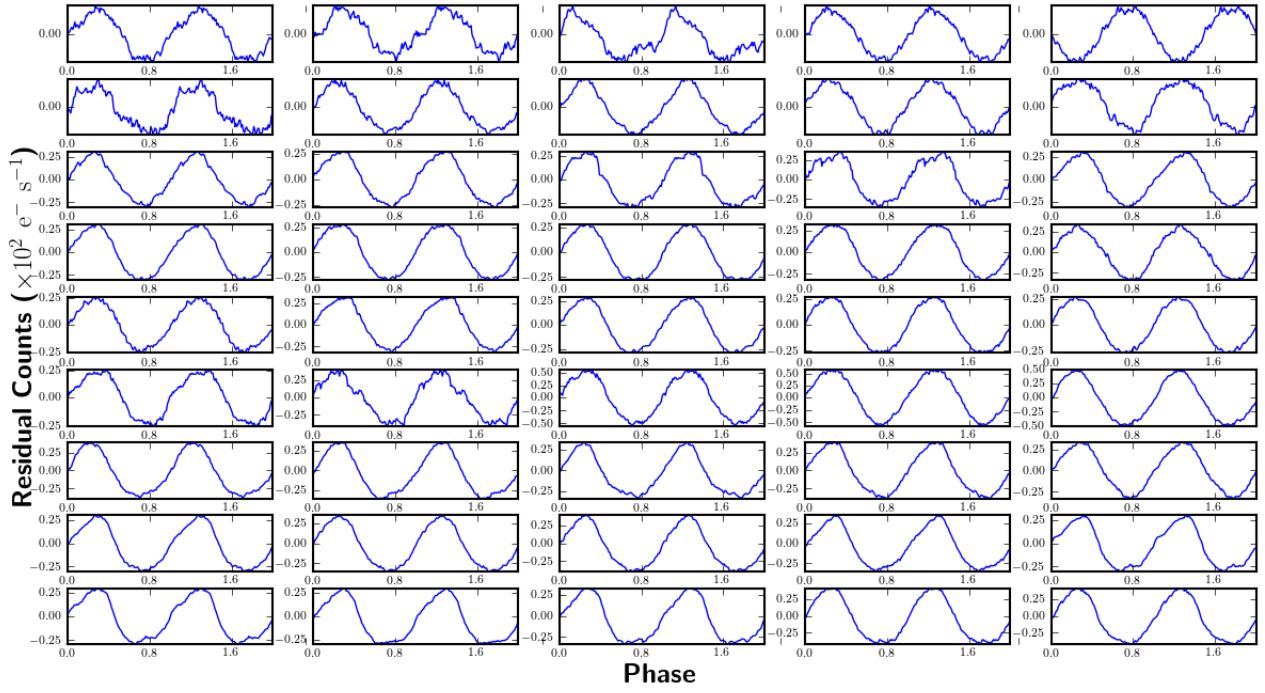


FIG. 16.— Negative superhump (Q6) V1504 Cyg